PMTJ Temperature Sensor utilizing VCMA

Abdelrahman G. Qoutb, *Student Member, IEEE* and Eby G. Friedman, *Fellow, IEEE*
Department of Electrical and Computer Engineering
University of Rochester
Rochester, New York 14627
a.qoutb@rochester.edu, friedman@ece.rochester.edu

***Abstract*—Thermal aware systems are able to control distributed CMOS blocks based on the local temperature to enhance system power, speed, and reliability. The ultimate objective is multiple *in situ* temperature sensors, close to the CMOS device layer, distributed over the die, physically small, and leaking almost zero power. Magnetic tunnel junctions (MTJ) are able to provide this capability. An MTJ is a CMOS compatible device, fabricated within the metallic layers, above the CMOS device layers. A method for using an MTJ as a thermal sensor is presented. The method operates MTJs in an antiparallel state where an MTJ is more sensitive to thermal variations as compared to the parallel state. The method exploits device magnetism, thermal stability, and resistance with respect to an applied sensing voltage to sense the ambient temperature. The results are based on experimentally extracted parameters of a perpendicular and voltage controlled magnetic anisotropy MgO|CoFeB MTJ. A change in the device antiparallel resistance of up to 16 Ω per degree Kelvin at a sensing voltage of 0.2 volts is exhibited.**

I. INTRODUCTION

The need for thermal aware systems is increasing. Systems able to measure the local ambient to affect system function are becoming increasingly desirable [1]. A thermal sensor near the CMOS device layer and sufficiently accurate to capture the local temperature is required. Materials with a high thermal conductivity and thermal stability are therefore desirable.

A thermal sensor is a two terminal device that produces an output current or voltage in relation to the ambient temperature. A thermal sensor should have low thermal mass and a fast response time. Integrated thermal sensors are monolithically fabricated in a semiconductor technology. These integrated thermal sensors are often in the form of bipolar junction transistors (BJT) where the relationship between the base-emitter voltage and collector-emitter current is a function of the ambient temperature. Recent developments have enabled the fabrication of stacked BTJs with a precision amplifier to enhance sensor accuracy [2].

A magnetic tunnel junction (MTJ) is a three layer structure composed of two ferromagnetic (FM) metallic layers separated by a nonmagnetic insulator layer. The tunneling magneto-resistance characterizes the change in device resistance based on the difference in orientation of the magnetization direction between the two FM layers [3]. The MTJ fabrication process is also CMOS compatible, fabricated within the IC metal layers.

This research is supported in part by the National Science Foundation under Grant Nos. CCF-1526466 and CCF-1716091, IARPA under Grant No. W911NF-17-9-0001, and by grants from Cisco Systems, Qualcomm, Synopsys, and Google.

MTJs are good candidates to become an effective temperature sensor since the MTJ resistance depends upon the ambient temperature [4], [5]. The device is small, CMOS compatible, close to the device layer, and leaks almost zero power. A network of MTJs, distributed over the die, can support local monitoring of the thermal characteristics across a system.

A mechanism is described here for using an MTJ in the antiparallel state as a thermal sensor based on a change in resistance with temperature. The antiparallel (AP) state is preferable for thermal sensing applications, as the parallel (P) state is almost independent of the ambient temperature. The paper is outlined as follows. In section II, the effects of temperature and voltage on the MTJ magnetic and electrical properties are discussed. A procedure for using an MTJ as a thermal sensor is described in section III. A case study of an MTJ-based thermal sensor is also described. In the case study, an electrical model is presented which is based on experimentally extracted parameters, as described in section IV. An MTJ-based thermal sensor circuit is presented in section V. The paper is concluded in section VI.

II. INFLUENCE OF TEMPERATURE AND VOLTAGE ON MTJ

MTJs are used as a memory element by pinning the magnetization of one of the FM layers while the other FM layer is the free magnetization layer. Both FM layers exhibit uniaxial magnetic anisotropy (MA) behavior, where a uniaxial preferably magnetization direction exists for the material magnetization. Two popular forms of FM materials used within an MTJ are in-plane MTJ (IMTJ) or out-of-plane perpendicular MTJ (PMTJ). IMTJs are elliptical structures where the shape anisotropy dominates the anisotropy behavior, resulting in magnetization along the long axis. PMTJs, alternatively, exhibit out-of-plane MA due to other forms of anisotropy, e.g., magneto-crystalline anisotropy or interfacial magnetic anisotropy [6].

An MTJ is used as a memory element by changing the state of the MTJ between parallel and antiparallel states, where both FM layers share the same orientation or are 180° out-of-phase. Changing the state of an MTJ is achieved by applying a torque with an energy greater than the system magnetization energy. The spontaneous magnetization energy is in the form of multiple magnetic anisotropies that exist within the FM system.

MTJs can be modeled as a bistable system, with two possible stable states, parallel and antiparallel. The energy separation between these states is controlled by the effective

978-1-7281-0397-6/19/$31.00 ©2019 IEEE

anisotropy energy ΔE. The system magnetization energy is a function of the device shape and physical dimensions in addition to the FM and tunneling (insulator) materials. The effective anisotropy energy ΔE is

$$\Delta E = K_{eff} v_{FM} = E_{Bulk\ anistropy} + E_{Interface\ anistropy} + E_{Demagnetization} + E_{VCMA}, \quad (1)$$

where K_{eff} is the effective anisotropy constant, and v_{FM} is the volume of the FM layer. ΔE can be approximated based on the MTJ structure, and E_{VCMA} is the energy maintained by the voltage controlled magnetic anisotropy (VCMA). Different forms of magnetic anisotropy can exist within the FM layers.

Recent studies have promoted PMTJs over IMTJs for high performance memory applications due to scalability, fast switching, and low power consumption for both writing and reading [7]. For a PMTJ, the perpendicular magnetic anisotropy (PMA) mechanism exists as either interfacial, bulk PMA, or both, based on the device material and shape. The anisotropy energy for a PMTJ without the voltage dependent term can be approximated as [8]

$$\Delta E|_{PMTJ} \approx [K_V + \frac{2K_i}{t_{FM}} - \frac{1}{2}\mu_0 (N_Z - N_{XY}) M_S{}^2] v_{FM}, \quad (2)$$

where K_V is the volume anisotropy constant, K_i is the surface interfacial anisotropy constant, t_{FM} is the thickness of the FM layer, μ_0 is the permeability of free space, N_Z is the demagnetization tensor in the $\hat{z}$ (perpendicular) direction, M_S is the saturation magnetization, and v_{FM} is the volume of the FM layer.

A. Influence of Voltage on MTJ

Some MTJ structures exhibit VCMA, where the applied voltage affects the magnetic anistropy of the MTJ. The effect of voltage on the MTJ can be modeled as a magnetic field $\vec{H}_{VCMA} = [2\zeta_{VCMA} V / \mu_0 M_S t_{ox} t_{FL}]\ \hat{e}_n$ normal to the MTJ structure, where ζ_{VCMA} is the VCMA coefficient, and V is the applied voltage [9]. The voltage dependent term of the anisotropy energy is modeled as [10]

$$\Delta E|_{VCMA} = \Delta E(0) - \frac{2\zeta_{VCMA} V A_{MTJ}}{t_{ox}}, \quad (3)$$

where $\Delta E(0)$ is the anisotropy energy with zero applied voltage, and A_{MTJ} is the surface area of the MTJ.

The tunneling magneto-resistance (TMR) characterizes the quality of the electrical response of the MTJ, where $TMR = (R_{AP} - R_P)/R_P$, R_{AP} is the antiparallel state resistance, and R_P is the parallel state resistance. TMR exhibits a voltage dependence, as shown in [11]

$$TMR(V) = \frac{TMR(0)}{1 + (V/V_h)^2}, \quad (4)$$

where $TMR(0)$ is the TMR at a zero applied voltage. According to the Juliere model, $TMR(0) = 2P_1P_2/(1 - P_1P_2)$, where P_1 and P_2 are the spin polarization percentage of the two FM layers, and V_h is the voltage at which TMR is halved [3].

B. Influence of Temperature on MTJ

R_P is independent of thermal variations, as experimentally described in [12]. The antiparallel resistance, however, decreases with an increase in temperature. The temperature influences most of the MTJ parameters, including the spin polarization $P(T)$, saturation magnetization $M_S(T)$, and all of the magnetic anisotropic constants $K(T)$, which affect the MTJ antiparallel resistance. $R_{AP} = 1/(G_{AP} \times A_{MTJ})$ where G_{AP} is the conductance of the AP state. The dependence of G_{AP} on temperature is

$$G_{AP}(T) = G_T [1 - P_1(T) P_2(T)\ ] + G_{SI}, \quad (5)$$

where $G_T = G_0\ (\sin(CT)/CT)$ is the elastic spin dependent term, $G_0 = \left(3.16 \times 10^{10} \sqrt{\phi_B}/t_{ox}\right) exp(-1.025 \times \sqrt{\phi_B} \times t_{ox})$ is the parallel state conductance at zero voltage and zero temperature, T is the ambient temperature, ϕ_B is the average tunneling barrier height (in eV), t_{ox} is the thickness of the insulator barrier layer, and $C = 1.387 \times 10^{-4} t_{ox}/\sqrt{\phi_B}$ is a material dependent parameter [13]. $G_{SI} = ST^{4/3}$ is the inelastic spin independent conductance, and S is a fitting parameter. The dependence of the spin polarization on temperature can be fitted as [14], [15]

$$P(T) = P(0) [1 - \beta_P T^{\alpha_P}\ ], \quad (6)$$

where β_P and α are fitting parameters related to the device dimensions and material properties.

The dependence of other MTJ parameters on temperature is primarily modeled by fitting expressions [16],

$$M_S(T) = M_S(0) \left[1 - \left(\frac{T}{T^*}\right)^{\beta_M}\right], \quad (7)$$

$$K_i(T) = K_i(0) \left(\frac{M_S(T)}{M_S(0)}\right)^{\beta_K}, \quad (8)$$

$$\zeta_{VCMA}(T) = \zeta_{VCMA}(0) \left(\frac{M_S(T)}{M_S(0)}\right)^{\beta_\zeta}, \quad (9)$$

where $P(0)$, $M_S(0)$, $K_i(0)$, and $\zeta_{VCMA}(0)$ are measured at zero temperature, and β and α are fitting factors for each parameter.

C. Combined Influence of Temperature and Voltage on MTJ

Using (4), (5), and (6), $TMR(T,V)$ can be described [17] by (10), and $R_{AP}(T,V)$ by (11).

$$TMR(T,V) = [\frac{TMR(0)}{1 + (V/V_h)^2}] \times \frac{2(1 - \beta_P T^\alpha)^2}{TMR(0)\left[1 - (1 - \beta_P T^\alpha)^2\right] + [1 + TMR(0)]\, G_{SI}/G_T + 2}, \quad (10)$$

$$R_{AP}(T,V) = R_P(TMR(T,V) + 1). \quad (11)$$

Using (2), (7), (8), and (9), the system anisotropy energy for a VCMA controlled PMTJ, neglecting the volume magnetic anisotropy term, is approximated as

$$\Delta E(T,V)|_{PMTJ} \approx [\frac{2K_i}{t_{FM}} - \frac{1}{2}\mu_0 (N_Z - N_{XY}) M_S{}^2 - \frac{2\zeta_{VCMA} V A_{MTJ}}{t_{ox}}] v_{FM}. \quad (12)$$

As previously mentioned, an energy barrier exists between the P and AP state. The device switches from the AP state to the P state when applying an energy that exceeds the built-in energy (related to the critical switching energy). The critical switching voltage, determined from (12), is

$$V_{C0}(T)|_{PMTJ} \approx \frac{t_{ox} t_{FM}}{\zeta_{VCMA}(T)} \left[\frac{K_i(T)}{t_{FM}} - \frac{1}{4}\mu_0 (N_z - N_{x,y}) M_S(T)^2 \right]. \tag{13}$$

III. MTJ-BASED THERMAL SENSOR

To sense the MTJ resistance, a voltage pulse is applied across the MTJ. To accurately measure the temperature, the change in the AP resistance due to an applied voltage and temperature needs to be determined. Equation (10) describes the maximum rate of change in the resistance with respect to temperature at the sensing voltage,

$$\max_{V_{min} \leq V \leq V_{max}} \left. \frac{\partial R_{AP}(T, V_i)}{\partial T} \right|_{V=V_i}, \tag{14}$$

where V_{min} and V_{max} are, respectively, the minimum and maximum voltage applied across an MTJ without changing the AP state.

The thermal stability Δ determines the limits of the applied voltage and the range of temperature where the device can stably operate. Δ is the ratio of the MTJ system magnetization energy and the energy perturbation to the system, which is a function of temperature and applied voltage,

$$\Delta(T, V) = \frac{\Delta E(T, V)|_{MTJ}}{K_B T} = \frac{K_{eff}(T, V) v_{FM}}{K_B T}, \tag{15}$$

where K_B is the Boltzmann constant. The bias point (the voltage pulse) can be determined from (13).

IV. CASE STUDY

The physical parameters used in this work are based on PMA and VCMA nanoscale MgO|CoFeB based MTJs [16], [17]. These physical parameters are listed in Table I.

TABLE I: MTJ physical parameters

Parameters	Description	Value
w_{FL}	FM width = radius	20 nm
t_{FL}	FM thickness	1.5 nm
t_{ox}	Barrier thickness	1.1 nm
Φ_{BL}	Barrier height	0.39 eV
V_h	Voltage @ half TMR	0.5 V
S	Spin independent conductance factor	1.1×10^{-12}
β_P	Fitting parameter for P	2.07×10^{-5}
α_P	Fitting parameter for P	2.3
β_M	Fitting parameter for M_S	1.5
T^*	Fitting parameter	1120 K
β_{Ki}	Fitting parameter	2.3
$\beta_{\zeta VCMA}$	Fitting parameter	2.83
N_z	Demagnetization tensor factor in Z	0.9343
N_{xy}	Demagnetization tensor factor in XY	0.015
K_{i0}	Interfacial MA at 0 K	$2.02 \times 10^{-3} J/m^2$
M_{S0}	Saturation magnetization at 0 K	$1457 \times 10^3 A/m$
TMR_0	TMR at 0 K	3
ξ_{VCMA0}	VCMA factor at 0 K	48.9×10^{-15} J/(V.m)

At a specific sensing voltage, the thermal stability of the device decreases with increasing temperature. The change in the thermal stability and antiparallel resistance when no sensing voltage is applied is depicted in Figure 2.

To characterize a read disturbance, the critical switching voltage, determined from (13), is 25.8 volts. The sensing voltage should therefore be less than half of that value, around 13 volts. In practical memory applications, to decrease the critical switching voltage, an embedded in-plane magnetic field bias is used [9], [18], or a polarizer layer is added to the MTJ structure [19]. Note that the device only operates due to VCMA. Other perturbation torques exerted by spin polarized electrons, such as spin transfer torque, are not considered.

An MTJ is evaluated under different scenarios to characterize the effect of the sense voltage and ambient temperature on the MTJ read disturbance. The magnetization behavior as a function of sense voltage with variable amplitude, pulse width of 10 ns, and ambient temperature of 300 K is illustrated in Figure 1a. The device exhibits a small disturbance but maintains the write state at a voltage below the predetermined critical switching voltage. As the sense voltage approaches the critical switching voltage, the read disturbance increases, as illustrated in Figures 1b and 1c.

The effect of thermal stability on the read disturbance and hence device sensitivity has also been evaluated. The device is evaluated with the same sense voltage, pulse width, but different ambient temperatures, as illustrated in Figures 1d and 1e. $\Delta(300, 5)$ is approximately 365, meaning the device energy is greater than the energy disturbance. In the second scenario, the same device is evaluated with the same sense voltage but with an ambient temperature of 600 K. Assuming the device maintains the same physical behavior at this high temperature, $\Delta(600, 5)$ is approximately 85. The device switches to the parallel state as the steady state is approached.

The simulations are based on a macrospin compact model with a 10 A/m external magnetic field in the $\vec{x}$ direction to evaluate the switching behavior. The simulation results for different scenarios of ambient temperature and voltage pulse amplitude are shown in Figure 1. Both the ambient temperature and/or the amplitude of the sense voltage are able to switch the device into the parallel state. The parallel state should be avoided to ensure the device remains sensitive to the ambient temperature.

The behavior of R_{AP} with respect to temperature and sense voltage is illustrated in Figure 3. At a specific sense voltage, the resistance decreases with respect to the ambient temperature. The rate of change in the resistance with respect to the sense voltage is illustrated in Figure 4. Operating an MTJ as a thermal sensor requires a sense voltage that can bias the device to the maximum rate of change in resistance with respect to the ambient temperature.

V. THERMAL SENSOR

The thermal sensor is shown in Figure 5a. The current amplifier enhances the sensitivity and amplifies any changes in the sense currents. R_{AP} can be measured as $R_{AP} = V_{sensing}/I_{sensing}$.

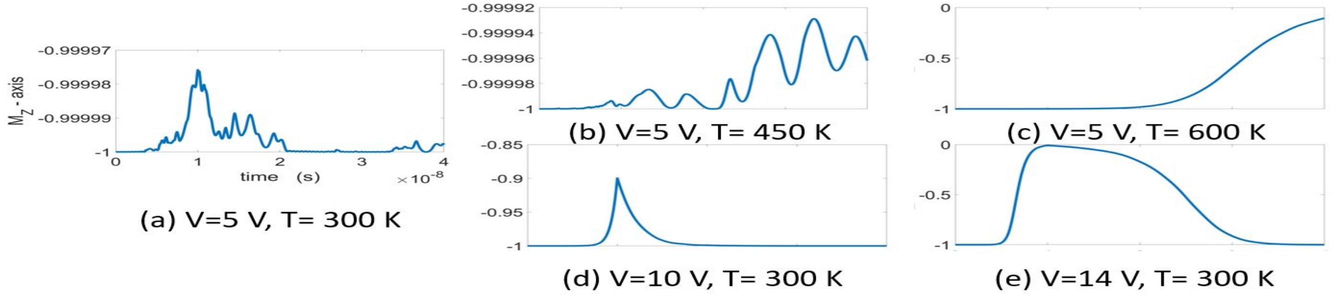

Fig. 1: Magnetization behavior of MTJ in Z-axis under different sense voltages V and ambient temperatures T, (a) V = 5 volts and ambient temperature T of 300 K, (b) V = 5 volts and T = 450 K, (c) V = 5 volts and T = 600 K, (d) V = 10 volts and T = 300 K, and (e) V =14 volts and T = 300 K

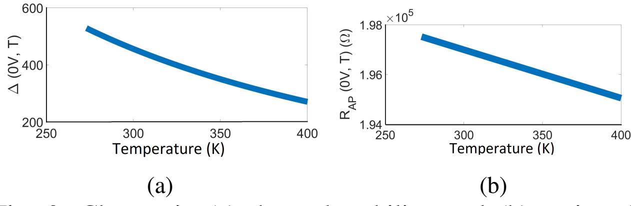

Fig. 2: Change in (a) thermal stability, and (b) antiparallel resistance with respect to temperature with no applied sense voltage

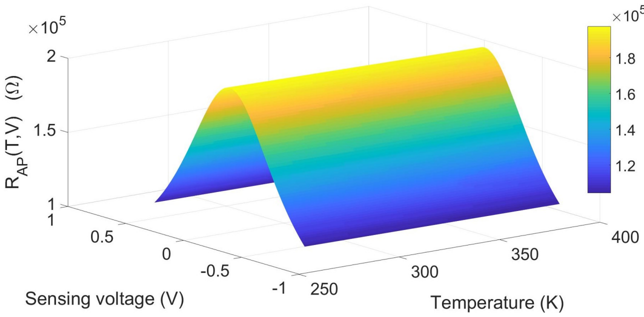

Fig. 3: Change in the antiparallel resistance with respect to temperature and voltage

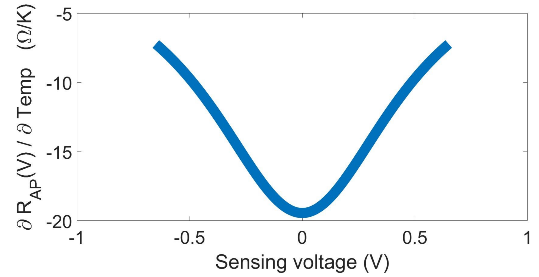

Fig. 4: Rate of change in the antiparallel resistance with respect to temperature and MTJ sense voltage

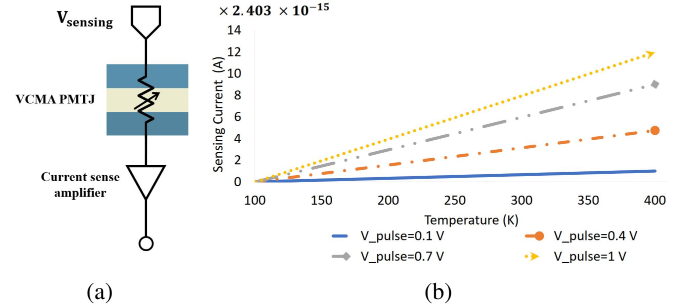

Fig. 5: Proposed thermal sensor, (a) thermal sensor circuit, and (b) thermal sense current for different sense voltages

VCMA-based MTJs can be used as a thermal sensor by applying a voltage pulse, and measuring the device resistance. The rate of change in the MTJ resistance with respect to temperature at around 0.2 volts is approximately 16 Ω per degree Kelvin, as illustrated in Figure 4. For multiple sense voltages, the rate of change in the normalized output current at an ambient temperature is shown in Figure 5b. For typical integrated sensors, a nominal output of 298 μA at 300 K with a change of 1 μA per degree Kelvin is exhibited.

An MTJ can be integrated above the CMOS device layer, providing high accuracy and local thermal access. An array of MTJs can be placed in series to increase the sensitivity of the sensor. Adding a distributed network of MTJs above the CMOS circuit blocks supports local monitoring of the system temperature. In addition, MTJ leaks almost zero current. The cost in standby power to support a thermal aware network is therefore low as compared to semiconductor-based thermal sensing techniques.

VI. CONCLUSIONS

A method is proposed for using an MTJ as a thermal sensor. The technique considers the effects of temperature and voltage on the thermal stability and resistance of an MTJ. Physical parameters, based on experimentally fabricated devices, are used to characterize the behavior of the MTJ. The MTJ can operate as a thermal sensor with a change in device resistance of up to 16 Ω per degree Kelvin at a sense voltage of 0.2 volts. A network of distributed MTJs can be used to efficiently monitor complex integrated systems to dynamically control local operation based on thermal and power constraints.

REFERENCES

[1] J. Zhou, T. Wei, M. Chen, J. Yan, X. S. Hu, and Y. Ma, "Thermal-Aware Task Scheduling for Energy Minimization in Heterogeneous Real-Time

MPSoC Systems," *IEEE Transactions on Computer-Aided Design of Integrated Circuits and Systems*, Vol. 35, No. 8, pp. 1269–1282, August 2016.
[2] T. Kuglestadt, "Semiconductor Temperature Sensors Challenge Precision RTDs and Thermistors in Building Automation," *Texas Instruments: Application Report: SNAA267–04*, pp. 2–10, 2015.
[3] M. Julliere, "Tunneling between Ferromagnetic Films," *Physics Letters A*, Vol. 54, No. 3, pp. 225–226, September 1975.
[4] Y. S. Chung, R. W. Baird, and M. A. Dulram, "Magnetic Tunnel Junction Temperature Sensors and Methods," U.S. Patent No. 7,510,883, June 2009.
[5] S. Schafer, D. Apalkov, A. V. Khvalkovskiy, V. Nikitin, R. Beach, and Z. Duan, "Method and System for Determining Temperature Using a Magnetic Junction," U.S. Patent Application No. 20160104544, April 2016.
[6] K. Yakushiji, T. Saruya, H. Kubota, A. Fukushima, T. Nagahama, S. Yuasa, and K. Ando, "Ultrathin Co/Pt and Co/Pd Superlattice Films for MgO-Based Perpendicular Magnetic Tunnel Junctions," *Applied Physics Letters*, Vol. 97, No. 23, pp. 232508, December 2010.
[7] A. G. Qoutb and E. G. Friedman, "MTJ Magnetization Switching Mechanisms for IoT Applications," *Proceedings of the Great Lakes Symposium on VLSI*, pp. 347–352, May 2018.
[8] B. Dieny, R. B. Goldfarb, and K. J. Lee, *Introduction to Magnetic Random-Access Memory*, Wiley, November 2016.
[9] J. G. Alzate Vinasco, *Voltage-Controlled Magnetic Dynamics in Nanoscale Magnetic Tunnel Junctions*, Ph.D. thesis, March 2014.
[10] W. Kang, Y. Ran, Y. Zhang, W. Lv, and W. Zhao, "Modeling and Exploration of the Voltage-Controlled Magnetic Anisotropy Effect for the Next-Generation Low-Power and High-Speed MRAM Applications," *IEEE Transactions on Nanotechnology*, Vol. 16, No. 3, pp. 387–395, May 2017.
[11] S. Zhang, P. M. Levy, A. C. Marley, and S. S.P. Parkin, "Quenching of Magnetoresistance by Hot Electrons in Magnetic Tunnel Junctions," *Physical Review Letters*, Vol. 79, No. 19, pp. 3744–3747, November 1997.
[12] Y. Wang, H. Cai, L. A.B. Naviner, Y. Zhang, J. O. Klein, and W. S. Zhao, "Compact Thermal Modeling of Spin Transfer Torque Magnetic Tunnel Junction," *Microelectronics Reliability*, Vol. 55, No. 9-10, pp. 1649–1653, August 2015.
[13] W. F. Brinkman, R. C. Dynes, and J. M. Rowell, "Tunneling Conductance of Asymmetrical Barriers," *Journal of Applied Physics*, Vol. 41, No. 5, pp. 1915–1921, April 1970.
[14] C. H. Shang, J. Nowak, R. Jansen, and J. S. Moodera, "Temperature Dependence of Magnetoresistance and Surface Magnetization in Ferromagnetic Tunnel Junctions," *Physical Review B - Condensed Matter and Materials Physics*, Vol. 58, No. 6, pp. R2917–R2920, August 1998.
[15] L. Yuan, S. H. Liou, and Dexin Wang, "Temperature Dependence of Magnetoresistance in Magnetic Tunnel Junctions with Different Free Layer Structures," *Physical Review B*, Vol. 73, No. 13, pp. 134403, April 2006.
[16] J. G. Alzate, P. K. Amiri, G. Yu, P. Upadhyaya, J. A. Katine, J. Langer, B. Ocker, I. N. Krivorotov, and K. L. Wang, "Temperature Dependence of the Voltage-Controlled Perpendicular Anisotropy in Nanoscale MgO|CoFeB|Ta Magnetic Tunnel Junctions," *Applied Physics Letters*, Vol. 104, No. 11, pp. 112410, March 2014.
[17] L. Zhang, Y. Cheng, W. Kang, L. Torres, Y. Zhang, A. Todri-Sanial, and W. Zhao, "Addressing the Thermal Issues of STT-MRAM From Compact Modeling to Design Techniques," *IEEE Transactions on Nanotechnology*, Vol. 17, No. 2, pp. 345–352, March 2018.
[18] M. Kazemi, E. Ipek, and E. G. Friedman, "Adaptive Compact Magnetic Tunnel Junction Model," *IEEE Transactions on Electron Devices*, Vol. 61, No. 11, pp. 3883–3891, June 2014.
[19] C. Y. You, "Reduced Spin Transfer Torque Switching Current Density with Non-Collinear Polarizer Layer Magnetization in Magnetic Multilayer Systems," *Applied Physics Letters*, Vol. 100, No. 25, pp. 1–5, June 2012.